Dual Function C-Terminal Domain of Dynamin-1: Modulation of Self-Assembly by Interaction of the Assembly Site with SH3 Domains†

Robin Scaife,‡ Catherine Vénien-Bryan,§ and Robert L. Margolis*

Institut de Biologie Structurale Jean-Pierre Ebel (CEA-CNRS), 41 avenue des Martyrs, 38027 Grenoble Cedex 1, France

Received May 19, 1998; Revised Manuscript Received September 21, 1998

ABSTRACT: Impairment of endocytosis by mutational targeting of dynamin-1 GTPases can result in paralysis and embryonic lethality. Dynamin-1 assembles at coated pits where it functions to cleave vesicles from donor membranes. Receptor endocytosis is modulated by SH3 (src homology 3) domain proteins, which directly bind to dynamin C-terminal proline motif sequences, affecting both the dynamin GTPase activity and its recruitment to coated pits. We have determined that dynamin−dynamin interactions, which are required for dynamin helix formation, involve these same SH3 domain-binding C-terminal proline motif sequences. Consequently, SH3 domain proteins induce the in vitro disassembly of dynamin helices. Our results therefore suggest the the dual function of the dynamin C-terminus (involving amino acids 800−840) permits direct regulation of dynamin assembly and function through interaction with SH3 domain proteins. Additionally, the N-terminal GTPase domain plays an important role in assembly. Finally, we show that the central PH (pleckstrin homology) domain exerts a strong inhibitory effect on the capacity for dynamin-1 self-assembly.

Intracellular vesicular transport is required for many cellular functions, ranging from axonal transport to endocytosis. Vesicle transport is in turn dependent on the biogenesis of intracellular vesicles such as endocytic vesicles from donor membranes. Formation of endocytic vesicles, which occurs by invagination and fission from the plasma membrane, generally involves the assembly of two distinct structures. First, clathrin assembles with associated adaptor proteins on the plasma membrane to form coated pits, which are then released from the plasma membrane as coated vesicles through the action of dynamin-1, which forms a helical, or horseshoe, shaped structure at the neck of deeply invaginated coated pits (*1*). Dynamin-1, a 100 kDa GTPase associated with a specific synaptosomal membrane fraction (*2*), is absolutely required for endocytosis. Expression of GTPase-defective dynamin-1 inhibits endocytosis of plasma membrane receptors (*3*−*5*) with consequences that can be severe. For example, mutations in shibire, a *Drosophila* homologue of dynamin, are lethal at the embryonic stage (*6*). In adult flies, ts shibire mutations result in rapid paralysis caused by depletion of synaptic vesicles at the neuromuscular junction (*7*−*9*).

Purified dynamin-1 self-assembles in vitro into horseshoe-shaped polymers, similar in size to the dynamin-1 containing helices observed in GTPγS-treated permeabilized synaptosomes (*10*). Thus, the helical structures that form at the necks of deeply invaginated coated pits in vivo appear to result from the self-assembly of dynamin-1 subunits (*1*). Addition of purified dynamin to liposomes has recently been demonstrated to induce the assembly of similar membranous tubules decorated with dynamin polymer (*11*,*12*). Although these dynamin-1 structures clearly have a central function in vesicle biogenesis, little is known regarding their assembly properties.

To determine what governs the self-assembly of dynamin-1, we have analyzed the involvement of these different dynamin-1 structural and functional domains in dynamin−dynamin interaction. We here present evidence for a critical involvement of specific C-terminal SH3 binding proline-rich motifs, the N-terminal GTPase domain, as well as the central PH domain, in dynamin−dynamin interactions. Further, proteins that contain SH3[1] domains appear to compete for the C-terminal proline-rich binding site, suggesting they play a controlling role in dynamin-1 assembly and disassembly at coated pits.

EXPERIMENTAL PROCEDURES

Two Hybrid Analysis. Human dynamin-1 cDNA (the "D-100-short" isoform) was subcloned into pGBT (Clontech), and ΔGTP, ΔPH, and ΔCOOH cDNA constructs were generated by restriction digestion of dynamin-1 cDNA with *Xho*I, *Sca*I−*Stu*I, or *Sma*I, respectively. Yeast strain SF526 (Clontech) was transfected with either pGBT-dynamin-1 or pGAD-dynamin-1 and verified by standard DNA sequencing protocols. Expression of dynamin-1 fusion proteins was

† This work was supported in part by grants (to R.L.M.) from the International Human Frontier Science Program (RG-513/94 M) and from IMABIO/ARC (6631).

* Author to whom correspondence should be addressed. Tel: (33) 4 76 88 96 16. Fax: (33) 4 76 88 54 94. E-mail: margolis@ibs.fr.

‡ Present address: Dept. of Pathology, Queen Elizabeth II Medical Centre, University of Western Australia, Monash Ave, Nedlands, 6009, Australia.

§ Present address: Laboratory of Molecular Biophysics, Rex Richards Building, Oxford University, South Parks Road, Oxford OX1 3QU, U.K.

[1] Abbreviations: PH domain, pleckstrin homology domain; SH3 domain, src homology 3 domain.

10.1021/bi981180g CCC: $15.00
Published on Web 12/02/1998

verified by anti-dynamin-1 Western blot, as previously described (*2*), of lysates derived from tryptophan or leucine auxotrophs, respectively. Sequences coding for dynamin-1 C-terminal fragments, generated by standard PCR methods using Vent polymerase (BioLabs), were subcloned (as *Bam*HI and *Eco*RI fragments) into pGBT or pGAD. Expression of gal4 DNA BD-dynamin-1 fragment fusion proteins was verified by anti-gal4 DNA-BD (Santa Cruz) Western blot of lysates derived from tryptophan auxotrophs. β-Galactosidase reporter gene activity was assayed quantitatively by measurement of OD_{420nm} development following incubation of cell lysates (obtained by two cycles of freeze−thawing) with 0.6 μg/mL ONPG substrate, and relative values were adjusted to take cell densities into account.

GST Fusion Proteins. Sequences coding for dynamin-1 C-terminal fragments were subcloned as *Bam*HI−*Eco*RI fragments into pGex-4T-3 (Pharmacia) and transformed into XL1Blue *Escherichia coli* (Stratagene). Ampicillin-resistant XL1Blue colonies were screened for expression of GST fusion proteins by anti-GST (Pharmacia) Western blot of cell lysates. GST fusion proteins were purified by glutathione-agarose affinity precipitation.

In Vitro Dynamin-1 Binding Assay. Purified dynamin-1 was obtained by DEAE-cellulose and ATP-affinity chromatography, as previously described (*2*), from clarified lysates of Sf21 cells that had been infected 68 h with recombinant baculovirus. Recombinant baculovirus was generated by transfection of Sf21 cells with pBakPac (Clontech) into which the dynamin-1 cDNA had been subcloned. Purified GST fusion proteins (at 8 μg/mL) were incubated overnight with purified dynamin-1 (at 10 μg/mL) and glutathione-agarose in 20 mM Hepes, pH 7.0, 50 mM NaCl, and 1 mM EGTA buffer (buffer A) containing 0.1% Triton X-100 and 0.5 mg/mL BSA. The glutathione-agarose was then washed four times with buffer A containing 0.1% Triton X-100 prior to treatment with SDS−PAGE buffer.

Electron Microscopy. Samples of dynamin-1, with and without GST-SH3 fusion proteins, were diluted to concentrations ranging 0.04−0.06 μg/mL in buffer A. Samples were applied to electron microscopy grids coated with carbon film and stained with 2% uranyl acetate for 30 s. The preparations were examined using a Zeiss 10 C electron microscope with an acceleration voltage of 80 kV. Electron micrographs were taken at a magnification of 40 000 under low-dose conditions.

Analytical Ultracentrifugation. Sedimentation experiments were carried out using dynamin-1 in buffer A. The sedimentation velocity experiments were performed at 10 °C using an Optima XL-A analytical ultracentrifuge from Beckman equipped with a four hole An-60 Ti rotor with double-sector of 1.2 cm path length, at 25 000 rpm. Twenty scans showing absorbance at 278 nm as a function of radial position were recorded at 3 min intervals.

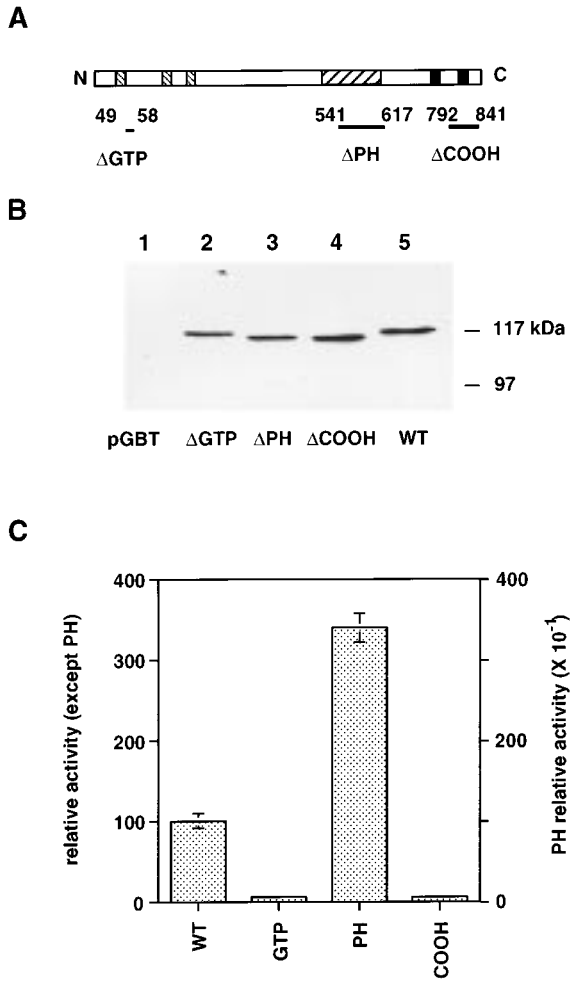

FIGURE 1: Two-hybrid analysis of dynamin−dynamin interaction domains. (A) Dynamin-1 is composed of an N-terminal GTPase domain, a central PH domain and C-terminal SH3 binding proline motif (PxxP) sequences, as indicated by hatched (GTPase and PH domains) or solid (proline-rich motifs) regions in the linear representation. There are multiple PxxP motifs, and this diagram only indicates their position, rather than number. Sequences deleted in dynamin-1 cDNA constructs, indicated by horizontal bars, correspond to amino acid positions 49−58 (ΔGTP), 541−617 (ΔPH), and 792−841 (ΔCOOH). The PH domain deletion represents removal of the functional region of the PH domain (*29*). (B) Dynamin-1 cDNA constructs were cloned into pGBT and expression of dynamin-1-gal4DNA-BD fusion proteins in yeast was determined by an anti-dynamin-1 Western blot of SDS−PAGE fractionated cell lysates following transfection with pGBT (lane 1), pGBT-dynaminΔGTP (lane 2), pGBT-dynaminΔPH (lane 3), pGBT-dynaminΔCOOH (lane 4), or pGBT-dynamin-1 (full-length) (lane 5). Molecular mass markers, corresponding to 117 and 97 kDa, are indicated. (C) Gal4DNA-BD-dynamin constructs were expressed in yeast cells transformed with gal4 DNA-AD-dynamin expressing plasmid. Relative activity of the gal4 promotor driven β-galactosidase reporter gene was determined quantitatively for each of the strains, as indicated (the ordinate values for the ΔPH construct are shown on the right scale).

RESULTS

Dynamin-1 contains several distinct structural and functional domains, including an N-terminal GTPase domain, a PH domain, and a proline-rich SH3 binding C-terminal region (Figure 1A). The PH (pleckstrin homology) domain represents a structural motif of approximately 100 amino acids, present in a number of proteins, where it has functions that include specific association with other proteins and with inositolphosphates (*13*). Proline motifs, of PxxP consensus sequence (*14*), associate specifically with SH3 (src homology 3) domains, which are conserved structural motifs involved in protein−protein interactions, originally identified in the src family of tyrosine kinases (*15*).

To determine what governs the self-assembly of dynamin-1, we have analyzed the involvement of these different

dynamin-1 structural and functional domains in dynamin−dynamin interaction. Dynamin-1 cDNAs containing deletions of portions of these domains were expressed as Gal4 DNA BD fusion proteins in yeast and could be detected by Western blot using anti-dynamin-1 serum (Figure 1B). Coexpression of these Gal 4 DNA BD fusion constructs with the dynamin-1 cDNA fused to the Gal4 DNA AD sequence has permitted a yeast two-hybrid analysis of the involvement of the deleted sequences in dynamin−dynamin interactions. The response is specific to the presence of dynamin-1 in both constructs. Thus, simultaneous expression of full-length dynamin-1 Gal4 fusion proteins from both the Gal4 DNA BD and the Gal4 DNA AD coding plasmids resulted in a strong β-galactosidase reporter gene signal (Figure 1C), while expression of dynamin-1 from only one of the Gal4 plasmids resulted in negligible β-galactosidase activity (data not shown).

Using this two-hybrid assay, we found that deletion of either dynamin-1 carboxyl terminal sequences (residues 792−841) or a sequence between elements I and II of the GTPase domain (residues 49−58) greatly reduced the signal of the dynamin−dynamin interaction dependent β-galactosidase reporter gene (Figure 1C). Surprisingly, deletion of the majority of the dynamin-1 PH domain from the Gal4 DNA BD fusion protein increased the β-galactosidase reporter gene signal by approximately 30-fold relative to full-length dynamin-1 (Figure 1C). We have found that purified PH domain deleted dynamin-1 readily self-assembles into horseshoe-shaped structures (data not shown). Similarly, it has recently been reported that dynamin-1 N- and C-terminal fragments readily self-assemble following removal of the PH domain by endoproteolytic cleavage and that the dynamin-1 PH domain may function as a negative regulator of GTP hydrolysis (*16*).

Since deletion of the C-terminal amino acid residues 792−841 appears to greatly decrease dynamin−dynamin interaction, we analyzed the dynamin-1-binding properties of the C-terminal portion of dynamin-1. Dynamin-1 C-terminal fragments were fused to either Gal4 DNA BD or Gal4 DNA AD (Figure 2A), and we expressed these fusion proteins in a yeast two-hybrid system. β-Galactosidase reporter gene activity was assayed to measure the interaction of these Gal4 DNA AD-dynamin-1 C-terminal fusion proteins with Gal4 DNA BD fused full-length dynamin-1. As anticipated, coexpression of Gal4 DNA AD-dynamin-1 C-terminal fusion proteins containing most of the dynamin-1 C-terminus with Gal4 DNA BD fused full-length dynamin-1 resulted in significant activity of the β-galactosidase reporter gene (Figure 2B). Fragments C-1 to C-3 are all approximately comparable, but are suppressed relative to full-length constructs. The fact that C-1 has lower activity than full-length dynamin-1 probably relates to the contribution of the N-terminus of dynamin-1 to self-association, as indicated in Figure 1.

In contrast to the longer C terminal fragments, expression of Gal4 AD fused to more extensively truncated C-terminal fragments (fragments C4 and C5) resulted in complete loss in the activity of the β-galactosidase reporter gene (Figure 2B). Deletion of dynamin-1 C-terminal residues 800−840 resulted in background activity levels of the β-galactosidase reporter gene, comparable to those obtained when Gal4 DNA BD-dynamin-1 or Gal4 DNA AD-dynamin-1 C-terminal fragments are coexpressed with Gal4 DNA AD or Gal4 DNA BD, respectively (Figure 2B).

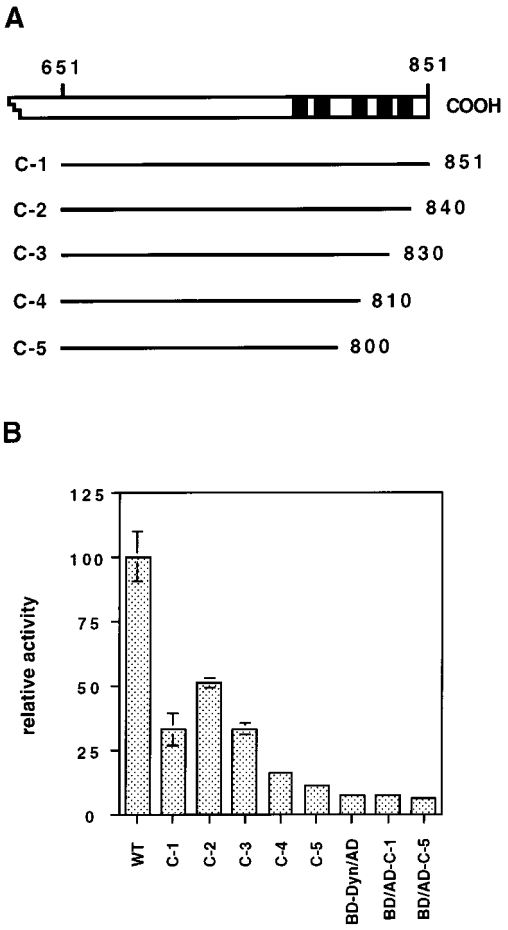

FIGURE 2: Two-hybrid analysis of the interaction of the dynamin-1 C-terminus with full-length dynamin-1. (A) The entire dynamin-1 C-terminus (fragment C-1, corresponding to amino acid residues 651−851) and four stepwise deletion constructs [fragments C-2 (amino acid residues 651−840), C-3 (residues 651−830), C-4 (residues 651−810), and C-5 (residues 651−800)] were generated by PCR. The filled boxes in the representation of the dynamin-1 C terminus represent the proline rich motifs. (B) Gal4-DNA-AD dynamin-1 cDNA constructs C-1 through C-5 were expressed in yeast transformed with plasmid expressing gal4DNA-BD-dynamin. Relative activity of the gal4 promotor driven β-galactosidase reporter gene was determined quantitatively for each of the strains, as indicated (BD, BD-Dyn, AD, AD-C-1, and AD-C-5 correspond to pGBT, pGBD-dyn, pGAD, pGAD-C-1, and pGAD-C-5, respectively).

Our yeast two-hybrid results indicated that dynamin-1 C-terminal sequences contribute to dynamin−dynamin interactions. We therefore wished to directly assay the dynamin-binding capability of the dynamin C-terminal region. Various dynamin-1 C-terminal sequences were hence expressed in *E. coli* as GST fusion proteins (Figure 3A) and their dynamin-1 binding was assayed following purification. Purified baculovirus-expressed dynamin-1 was incubated with glutathione-agarose immobilized GST-dynamin-1 C-terminal fragments. Bound dynamin-1 was detected following SDS−PAGE and Western blotting with anti-dynamin-1 serum. Using this assay, we found that a GST fusion protein containing dynamin-1 amino acid residues 651−851 can indeed bind dynamin-1 in vitro (Figure 3B). This in vitro interaction appears to be quite weak, however, since only a small fraction of the total dynamin pool bound

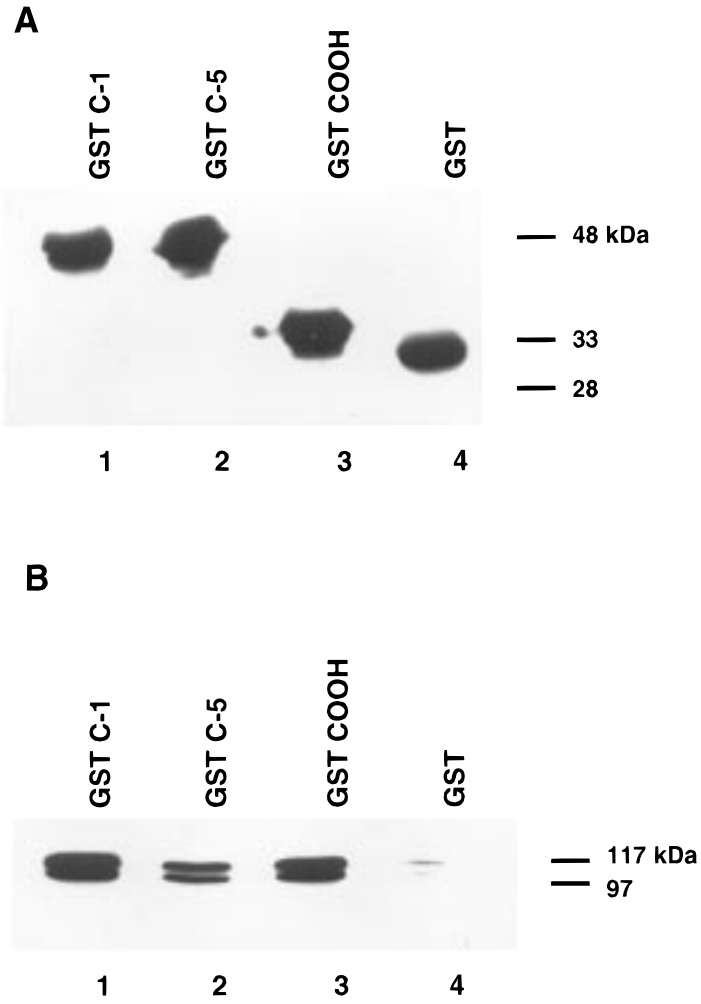

FIGURE 3: Binding of dynamin-1 to bacterially expressed dynamin-1 C-terminal fragment. (A) Anti-GST Western blot of cell lysates derived from XL1Blue bacteria transformed with pGex plasmid containing sequence for the entire dynamin-1 C-terminus (GST-C-1, corresponding to dynamin-1 amino acid residues 651−851, lane 1), dynamin-1 residues 651−800 (GST C-5, lane 2), dynamin-1 residues 801−840 (GST COOH, lane 3) or GST (lane 4). Molecular mass markers, corresponding to 48, 33, and 28 kDa, are indicated. (B) Dynamin-1 was incubated with glutathione-agarose immobilized GST dynamin-1 C-terminal fragments C-1, C-5, C-COOH, or GST, and glutathione-agarose-associated proteins were subjected to SDS−PAGE and anti-dynamin-1 Western blot. Lane 1, GST C-1; lane 2, GST C-5; lane 3, GST COOH; lane 4, GST. Molecular mass markers, corresponding to 117 and 97 kDa, are indicated. Dynamin appears as a doublet band, possibly as a result of proteolysis of C-terminal residues. Some proteolysis may have resulted from storage of dynamin at 4 °C. Such storage conditions were necessary since we have found that freezing of dynamin completely inactivates subsequent dynamin−dynamin interactions.

to the immobilized dynamin C-terminus fragment (data not shown).

Two-hybrid analysis of dynamin−dynamin interactions indicated that dynamin-1 residues 800−840 are important for dynamin−dynamin interaction. In vitro binding analysis supports this result. Above, we showed that removal of these residues by truncation of the dynamin-1 C-terminus GST fusion protein at amino acid residue 800 diminished its ability to bind dynamin-1 (Figure 2B). To further investigate the dynamin-1-binding properties of dynamin-1 amino acid residues 800−840, we expressed this short segment of dynamin-1 as a GST fusion protein. Strikingly, we found that this short GST fusion protein (containing dynamin-1 residues 800−840) binds dynamin-1 (Figure 3B) at a level similar to that found with the larger dynamin-1 C-terminal fragment C-1 (amino acid residues 651−851). Therefore, we have demonstrated that a short deletion of the C-terminus containing proline-rich motifs greatly reduces dynamin−dynamin interaction, while almost precisely the same sequence has dynamin-1 binding activity when expressed and assayed in vitro.

The C-terminal dynamin-1 sequence that appears to be involved in dynamin−dynamin interactions contains several SH3 domain binding proline motifs (Figure 1A). We therefore wished to determine whether dynamin−dynamin interaction, or dynamin-1 self-assembly, is perturbed by binding of SH3 domain proteins to the dynamin-1 C-terminal sequences. Dynamin−dynamin self-association can be directly observed by electron microscopy of purified dynamin-1 samples. Purified dynamin-1 self-associates into horseshoe-shaped structures (Figure 4A) and occasionally into helical superstructures (Figure 4D). While addition of GST alone has no effect on these structures (Figure 4C), we found that addition of purified GST-SH3 domain of Grb2 (Figure 4B) and of PLCγ, p85-SH3, and src (data not shown) caused these horseshoe-shaped structures to disassemble. The apparent disassembly induced by SH3 domain, as observed by electron microscopy, was confirmed by quantitative

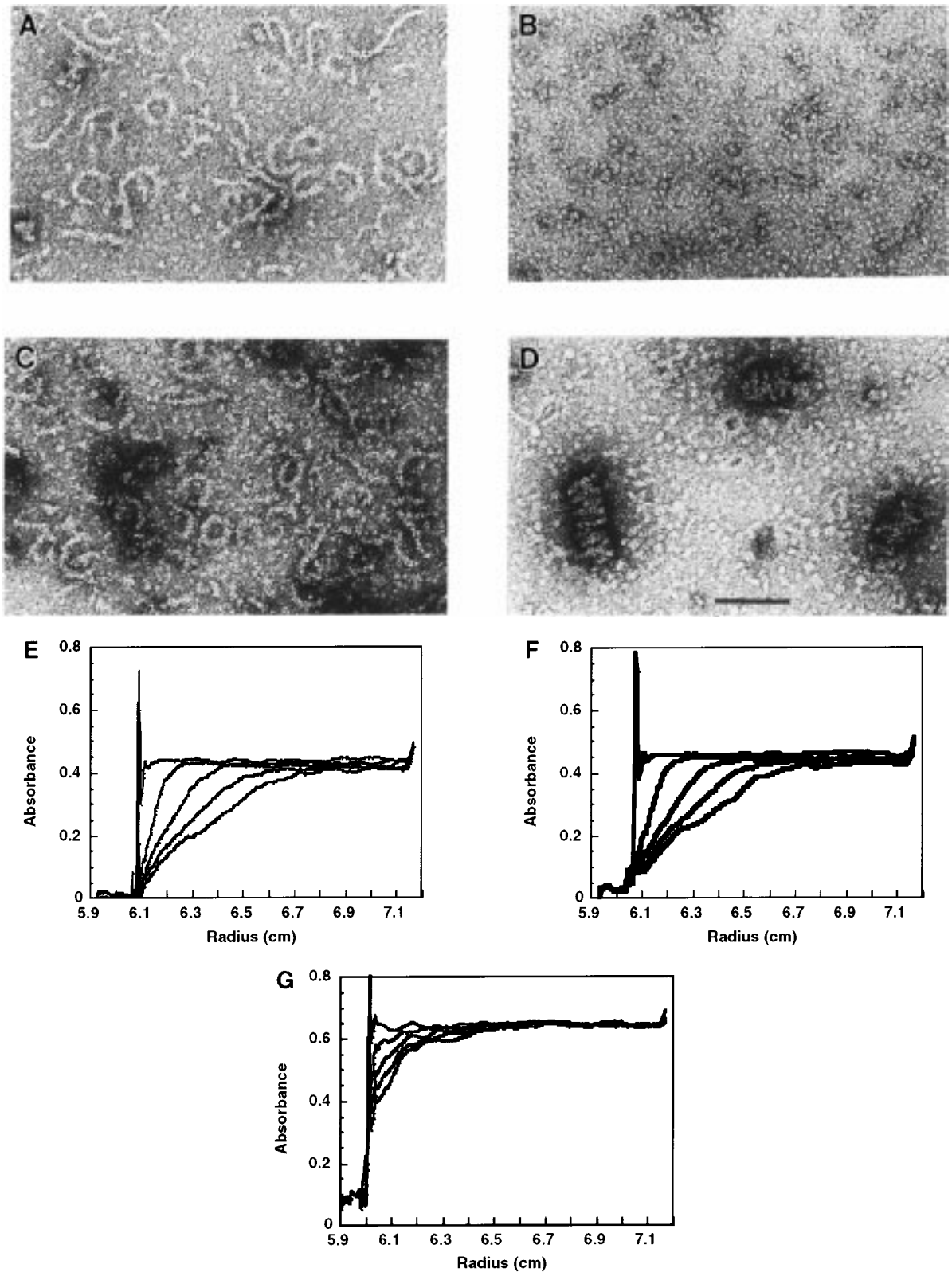

FIGURE 4: SH3 protein induced disassembly of dynamin-1 polymers. Negative stain electron microscopy images of (A) dynamin-1 (at 0.06 mg/mL), (B) dynamin-1 in the presence of GST fused to the Grb2 C-SH3 domain (0.1 mg/mL), (C) dynamin-1 in the presence of GST alone (0.1 mg/mL), and (D) occasional helical superstructures formed during control dynamin-1 assembly. The bar represents 100 nm. Incubation of samples for electron microscopy was done at room temperature in 20 mM Hepes, pH 7.0, 50 mM NaCl, and 1 mM EGTA. No Mg^{2+} or GTP was included in the incubation. (E−G) Analytical ultracentrifugation analysis of dynamin-1 disassembly. (E) Time course of sedimentation of assembled dynamin-1 (s20,w = 32 S), (F) Time course of sedimentation of assembled dynamin-1 exposed to 1:10 ratio of GST-Grb2 C-SH3 domain. There is no significant shift from the mass of dynamin-1 alone. (G) Time course of dynamin-1 sedimentation in the presence of stoichiometric amounts of GST-Grb2 C-SH3 domain (s20,w = 7 S). Sedimentation profiles after 0, 10, 25, 40, and 55 min of centrifugation at 42 000 rpm at 10 °C are shown from left to right. Similar results for both electron microscopy and analytical ultracentrifugation were also obtained with SH3 domains of PLCγ, p85, and src.

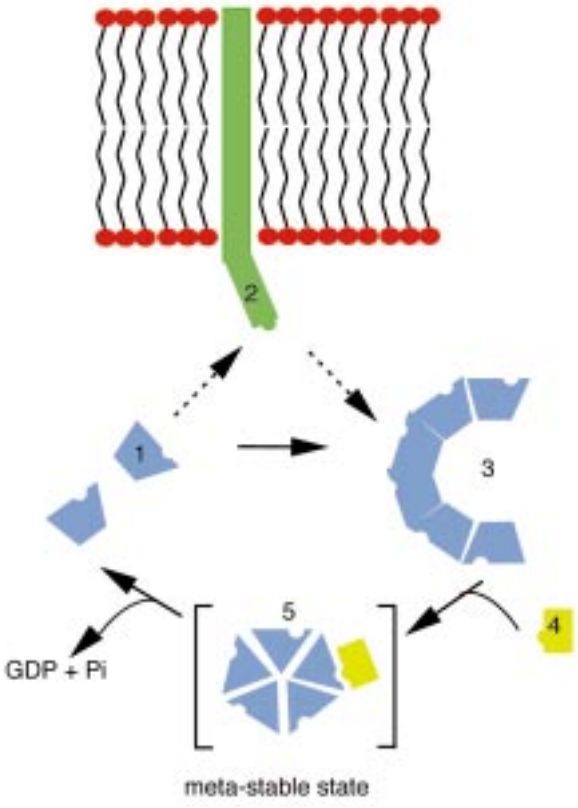

FIGURE 5: A model for the involvement of SH3 domain proteins in dynamin-1 function. Dynamin subunits (1) may be recruited to the plasma membrane in an unassembled form by amphiphysin (2) (*30*), where they subsequently assemble into collars around invaginated pits (3). Binding of SH3 proteins (4) destabilizes the polymer by disrupting dynamin−dynamin interactions, resulting in a conformational change in the polymer (5). This conformational change, which may permit the scission of the neck of the nascent coated vesicle, is followed by GTPase-dependent fragmentation of the metastable polymer.

analytical ultracentrifugation, which revealed a strong shift in mass on addition of a stoichiometric level of Grb2 C-SH3 to assembled dynamin-1 (Figure 4, panels E−G). The assembled form (Figure 4E) migrated with a calculated sedimentation coefficient of 32 S, equivalent to between an M_r of (2 and 3) $\times$ 10^6, assuming an elongated structure (we also resolve a minor peak representing approximately 5% of the protein, which migrates at 6 S), whereas dynamin-1 treated with stoichiometric amounts of GST-SH3 (Figure 4G) migrated at 7 S, equivalent to an M_r of approximately 1.3 $\times$ 10^5 and consistent with a monomer bound to GST-SH3. A ratio of Grb2 C-SH3 10-fold lower than dynamin resulted in no significant shift in mass of the assembled structure (Figure 4F).

DISCUSSION

In this study, we analyzed dynamin−dynamin interactions, which are required for self-assembly of dynamin-1 into helical structures that appear to be required for biogenesis of endocytic or synaptic vesicles (*1*,*10*). In a yeast two hybrid system using β-galactosidase as the reporter gene, dynamin-1 was expressed either as a gal4 DNA BD fusion protein or as a gal4 AD DNA AD fusion protein. Dynamin−dynamin interactions can readily be detected in this system. For example, β-galactosidase signal develops within minutes in yeast strains expressing both of the gal4-dynamin-1 fusion constructs. Such a strong dynamin−dynamin interaction is expected in light of the ability of dynamin-1 to form a stable protein superstructure.

We have found that either deletion of a small segment of the dynamin-1 GTPase domain (between elements I and II) or deletion of a portion of the dynamin-1 C-terminal proline-rich sequence greatly diminishes dynamin−dynamin interactions. The dynamin-1-related anti-viral Mx also self-assembles into horseshoe-shaped structures (*17*). Mx protein sequence between elements I and II of the GTPase domain appears to be required for homologous interaction between Mx proteins, and our results show that dynamin-1 has a similar requirement. The effect of deleting this portion of the GTPase domain on the overall structure or folding of these proteins has not been established. These results are supported by in vitro binding assays, in which dynamin-1 binds to a GST fusion protein linked to the dynamin-1 GTPase domain (RMS and RLM, unpublished observations). Our results indicate that both the GTPase domain and the proline-rich motif are required for dynamin-1 assembly. It remains to be determined if this dual requirement results from a cooperative binding interaction between these two sites.

It has previously been reported that removal of the dynamin-1 C-terminus by limited proteolysis abolishes its ability to self-assemble in the absence of phospholipid (*10*). In agreement with this study, our results demonstrate that the dynamin-1 C-terminal proline-rich sequences have a direct role in dynamin−dynamin interactions. Expression of gal4 AD fused with dynamin-1 C-terminal fragments gave rise to a significant β-galactosidase signal when coexpressed with gal4 BD-dynamin-1. Further, bacterially expressed GST-dynamin-1 C-terminal fragments are able to bind in vitro to purified dynamin-1. By stepwise deletion analysis, we identified the portion of the dynamin-1 C-terminus involved in homologous interactions. Surprisingly, our results indicated that amino acid residues 800−840, which have previously been identified as specific SH3 domain binding sites (*18*,*19*), correspond to the dynamin−dynamin interaction site. This finding suggested that binding of SH3 domain proteins to proline motifs that lie between amino acid positions 800 and 840 could directly interfere with the dynamin−dynamin interactions that occur at this site. Dynamin-1 has been demonstrated to interact with several SH3 domain proteins in vivo (*19*−*21*). For example, dynamin-1 forms a complex with Grb2 in CHO-IR cells, both before and after insulin activation (*22*). Further, in MDCK cells, microinjection of a Grb2 SH3 domain impairs EGF-receptor internalization (*23*) while microinjection of the amphiphysin SH3 domain into lamprey synapses prevents synaptic vesicle biogenesis by coated vesicle fission from the plasma membrane (*24*). These results clearly demonstrate that SH3 domain proteins may modulate the biological activity of dynamin-1. Our results suggest that one means by which they do so is through interference with dynamin−dynamin interaction.

Deletion of the SH3 domain binding sequence from amino acid residue 785 to 851 was found to abolish colocalization of dynamin-1 with clathrin coated pits (*25*). Further, Wigge et al. (*26*) have demonstrated that the SH3 domain of amphiphysin, which binds to residues 827−839 of dynamin (*18*), specifically inhibits endocytosis. These results could reflect a requirement for interaction with an SH3 domain

protein in order to localize dynamin to coated pits. Our results indicate that these same sequences contribute to dynamin−dynamin interactions. It is hence possible that involvement of these C-terminal sequences in dynamin localization to coated pits may reflect a requirement for dynamin oligomerization before binding to coated pits.

Our results indicate that the C-terminal proline-rich domain of dynamin-1 from amino acid 800 to 840 can either bind to another dynamin-1 subunit or can associate with an SH3 domain, but it cannot do both simultaneously. These results demonstrate that sequences in the proline-rich domain, though not necessarily overlapping, have at least two distinct binding functions. It is reasonable to conclude that these mutually exclusive binding functions indicate a controlling role in the availability of this site for dynamin-1 self-association. The SH3 protein required for delivery of dynamin-1 to a receptor may thus serve also to prevent its premature assembly. At the point when the assembled dynamin-1 must cleave the neck of the budding vesicle, reassociation of an SH3 protein can both stimulate the necessary GTPase activity and induce the conformational changes necessary for the ordered disassembly of the helical dynamin-1 structure that is required for the scission event (*11*).

In addition to demonstrating a role for the dynamin-1 C-terminus in dynamin−dynamin interactions, our results indicate a potential regulatory role for the dynamin-1 PH domain in dynamin-1 self-association. PH domains have previously been reported to function in homologous protein interactions. In the case of the signal transducing kinase akt, the PH domain appears to be required for dimerization (*27*). It has recently been suggested that the PH domain plays an important regulatory role in dynamin-1 GTPase activity (*16*). Our results with dynamin-1 complement these results and indicate that the dynamin-1 PH domain may play an important negative regulatory role in dynamin−dynamin interactions, and hence also in dynamin-1 self-assembly. Deletion of the dynamin-1 PH domain does not appear to affect the overall conformation or folding of the protein since PH domain deleted dynamin-1 retains SH3 domain activated GTPase activity (*28*). In contrast, we found that deletion of the dynamin-1 PH domain greatly augments the dynamin−dynamin interaction. The assembly of dynamin-1 may hence be regulated by PH domain ligands such as phosphatidyl inositols, which are generated upon receptor tyrosine kinase activation. Recent data indicate a major role for phosphorylation in regulating the interaction between dynamin-1 and the SH3 protein amphiphysin (*29*). This raises the possibility of further physiological controls that may modulate the switch between dynamin-SH3 protein binding and dynamin−dynamin assembly. Additional work will be required to further explore these intriguing possibilities and to firmly establish the regulatory mechanisms involved in the complex series of events that take place between SH3 proteins and the dynamin-1 C-terminus during dynamin-1 self-assembly and endocytosis.

ACKNOWLEDGMENT

We thank Dr. Christine Ebel for expert help with analytical ultracentrifugation and Dr. Richard Wade for use of his electron microscopy facility, Dr. Sandra Schmid and Dr. Ivan Gout for generously supplying human dynamin-1 cDNA and GST-SH3 fusion proteins, respectively. We are also indebted to Evelyne Gout for assistance in the generation of recombinant dynamin-1 expressing baculovirus. This is publication no. 551 of the Institut de Biologie Structurale Jean-Pierre Ebel.

REFERENCES

1. Takei, K., McPherson, P. S., Schmid, S. L., and De Camilli, P. (1995) *Nature 374*, 186−190.
2. Scaife, R., and Margolis, R. L. (1990) *J. Cell. Biol. 111*, 3023−3033.
3. Damke, H., Baba, T., Warnock, D. E., and Schmid, S. L. (1994) *J. Cell. Biol. 127*, 915−934.
4. Herskovits, J. S., Burgess, C. C., Obar, R. A., and Vallee, R. B. (1993) *J. Cell. Biol. 122*, 565−578.
5. van der Bliek, A. M., Redelmeier, T. E., Damke, H., Tisdale, E. J., Meyerowitz, E. M., and Schmid, S. L. (1993) *J. Cell. Biol. 122*, 553−563.
6. Poodry, C. A., Hall, L., and Suzuki, D. T. (1973) *Dev. Biol. 32*, 373−386.
7. Poodry, C. A., and Edgar, L. (1979) *J. Cell. Biol. 81*, 520−527.
8. Ikeda, K., Ozawa, S., and Hagiwara, S. (1976) *Nature 259*, 489−491.
9. Siddiqi, O., and Benzer, S. (1976) *Proc. Natl. Acad. Sci. U.S.A. 73*, 3253−3257.
10. Hinshaw, J. E., and Schmid, S. L. (1995) *Nature 374*, 190−192.
11. Sweitzer, S. M., and Hinshaw, J. E. (1998) *Cell 93*, 1021−1029.
12. Takei, K., Haucke, V., Slepnev, V., Farsad, K., Salazar, M., Chen, H., and De Camilli, P. (1998) *Cell 94*, 131−141.
13. Shaw, G. (1996) *Bioessays 18*, 35−46.
14. Yu, H., Chen, J. K., Feng, S., Dalgarno, D. C., Brauer, A. W., and Schreiber, S. L. (1994) *Cell 76*, 933−945.
15. Koch, C. A., Anderson, D., Moran, M. F., Ellis, C., and Pawson, T. (1991) *Science 252*, 668−674.
16. Muhlberg, A, D. Warnock, D., and Schmid, S. L. (1997) *EMBO J. 16*, 6676−6683.
17. Nakayama, M., Nagata, K., Kato, A., and Ishihama, A. (1991) *J. Biol. Chem. 266*, 21404−21408.
18. Okamoto, P. M., Herkovits, J. S., and Vallee, R. B. (1997) *J. Biol. Chem. 272*, 11629−11635.
19. Scaife, R., Gout, I., Waterfield, M. D., and Margolis, R. L. (1994) *EMBO J. 13*, 2574−2582.
20. Seedorf, K., Kostka, G., Lammers, R., Bashkin, P., Daly, R., Burgess, W. H., van der Bliek, A. M., Schlessinger, J., and Ullrich, A. (1994) *J. Biol. Chem. 269*, 16009−16014.
21. Miki, H., Miura, K., Matuoka, K., Nakata, T., Hirokawa, N., Orita, S., Kaibuchi, K., Takai, Y., and Takenawa, T. (1994) *J. Biol. Chem. 269*, 5489−5492.
22. Ando, A., Yonezawa, K., Gout, I., Nakata, T., Ueda, H., Hara, K., Kitamura, Y., Noda, Y., Takenawa, T., Hirokawa, N., et al. (1994) *EMBO J. 13*, 3033−3038.
23. Wang, Z., and Moran, M. (1996) *Science 272*, 1935−1939.
24. Shupliakov, O., Low, P., Grabs, D., Gad, H. H. C., David, C., Takei, K., De Camilli, P., and Brodin, L. (1997) *Science 276*, 259−263.
25. Shpetner, H. S., Herskovits, J. S., and Vallee, R. B. (1996) *J. Biol. Chem. 271*, 13−16.
26. Wigge, P., Vallis, Y., and McMahon, H. T. (1997) *Curr. Biol. 7*, 554−560.
27. Datta, K., Franke, T. F., Chan, T. O., Makris, A., Yang, S. I., Kaplan, D. R., Morrison, D. K., Golemis, E. A., and Tsichlis, P. N. (1995) *Mol. Cell. Biol. 15*, 2304−2310.
28. Salim, K., Bottomley, M. J., Querfurth, E., Zvelebil, M. J., Gout, I., Scaife, R., Margolis, R. L., Gigg, R., Driscoll, P. C., Waterfield, M. D., and Panayotou, G. (1996) *EMBO J. 15*, 6241−6250
29. Slepnev, V. I., Ochoa, G.-C., Butler, M. H., Grabs, D. and De Camilli, P. (1998) *Science 281*, 821−824.
30. Owen, D. J., Wigge, P., Vallis, Y., Moore, J. D. A., Evans, P. R., and McMahon, H. T. (1998) *EMBO J. 17*, 5273−5285.

BI981180G